

Supplementary Information to Investigating Structure and Dynamics of Unentangled Poly(dimethyl-co-diphenyl)siloxane via Molecular Dynamics Simulation

Weikang Xian,[†] Jinlong He,[†] Amitesh Maiti,[‡] Andrew P. Saab,[‡] and Ying Li*,[†]

[†]*Department of Mechanical Engineering, University of Wisconsin-Madison, Madison, WI
53706-1572, United States*

[‡]*Lawrence Livermore National Laboratory, Livermore, California 94550, United States*

E-mail: yli2526@wisc.edu

Phone: 608 265 0577. Fax: 608 890 3966

Sequences of the Copolymer All the chains in a system with particular ϕ share the same sequence as mentioned in the main text. All the sequences are given in Table S1.

Table S1: Cooling rates in the simulation to estimate density-temperature relation.

Molar ratio ϕ	Sequence
0.2	1011000000 0101000000 0001001000 0000000001 0000000011
0.3	0011001001 0101001110 1001010000 0010010010 0000000000
0.4	1111001000 0111001110 0001001110 1100000001 1001000000
0.6	0001011100 1111101010 1100010101 1101010111 0111101011

Structural Properties Rescaled mean-squared end-to-end distances of the configurations from the beginning and the ending stages of the production runs at 550 K are shown in Fig.

S1. The results were calculated based on ten configurations with a time interval of 0.2 ns that was selected from the beginning stage and the ending stage for each molar ratio. The minor differences between the beginning and the ending stages indicate that the production runs are indeed started with equilibrium configurations.

Additionally, we extracted the properties of the PDMS from our MD simulation and compared them with results from experimental studies. The total structural factor $H(k)$ was calculated according to the detailed method and then compared with the result from wide-angle X-ray scattering experiment.^{1,2} The comparison is shown in Fig. S2. In addition, RDFs were also compared as shown in Fig. S3. The agreement in the comparisons confirms that our MD simulation protocol indeed captures the structural properties of the PDMS. It is worth noting that our MD results are shown in Fig. S2 and Fig. S3 were calculated at 298 K with 100 20-mers in total. A system of 100 50-monomer chains was also simulated at 298 K. Sufficient long production run times were used to fully equilibrate the two systems, as shown in Fig. S4 with the horizontal dashed lines representing the respective mean-squared end-to-end distance of the two systems. The characteristic ratio C was estimated according to $\langle R_{ee}^2 \rangle = Cnl^2$ where n and $l = 1.65 \text{ \AA}$ are the numbers and the bond length of silicon-oxygen bond along the backbone respectively. The evaluated values are 5.52 ± 0.25 and 6.41 ± 0.25 for $N=20$ and $N=50$ systems respectively, as shown in Fig. S5. The results were averaged by 100 distinct trajectories with a 0.1 ns time lag. As a comparison, the values of 6.16 and 6.36 were reported for conditions of 298 K and 413 K for entangled melts according to Eq. 21 and Eq. 25 in the reference,³ while the value of 5.28 from the simulation was reported by Tzounis et al.⁴

Thermal Properties We probed the glass transition temperatures T_g of four systems as given in Fig. S6. We adopted the model from literature⁵ to fit the density-temperature curves such that we can estimate the glass transition temperature from the fitting parameters. The values of T_g are indicated by the dash lines and clearly marked. The density-temperature

isobars were acquired by running molecular dynamics in NPT ensembles with the same setting parameters detailed in the main text except the temperature was cooled from high to low temperature with cooling rate detailed in Table S2. In addition, the estimated values of T_g were also compared with experimental values⁶⁻⁹ as shown in Fig. S7, dashed line is computed by the Fox equation.¹⁰ Although the T_g value predicted by MD simulation is usually overestimated,¹¹ a qualitative agreement suggested by the comparison confirms that our MD simulations can reasonably capture the density-temperature dependency. In addition, the thermal expansion coefficient α of PDMS was also evaluated by fitting the high-temperature section of the density-temperature relation in Fig. S6 (a). The fitted values of $8.91 \times 10^{-4} \text{ K}^{-1}$ at 298 K, consistent to experimentally measured value of $9.07 \times 10^{-4} \text{ K}^{-1}$.¹²

Table S2: Cooling rates in the simulation to estimate density-temperature relation.

Molar ratio ϕ	0	0.2	0.4	0.6
Cooling rates	67 K/ns	80 K/ns	100 K/ns	100 K/ns

Mean-Squared Displacement The detailed mean-squared displacements, g_1 and g_3 , of all five systems at 550 K are shown in the Fig. S9. g_3 is defined in the main text Eq. 2, representing the MSD of the CM of the polymer chains. g_1 has a similar definition but it is defined based on the MSD of the monomers. It is defined in Eq. S1 where the angle bracket represents averaging over all the chains and the ensemble.

$$g_1(t) \equiv \langle [\mathbf{R}_i(t) - \mathbf{R}_i(0)]^2 \rangle \tag{S1}$$

Upon full relaxation, the g_1 and g_3 overlap, and they both scale with time linearly. They entered the diffusion regime as most of the mean-squared displacements exceeded the respective mean-squared end-to-end distances except in the case of $\phi = 0.6$ where only the g_1 exceeded the mean-squared end-to-end distance while g_3 was close to satisfy the criteria.

Normal Mode Analysis The auto-correlation of normal modes was calculated according to Eq. 9 in the main text. The decays are shown in Fig. S10 with best fits according to Eq. 10. The effective relaxation times are marked as well.

Dynamic Structure Factor In Fig. 8 in the main text, the predictions of the dynamic structure factor are compared with the ones calculated from the trajectories generated by the molecular simulation and there is no extra fitting involved. To extract the friction coefficients for the Kuhn monomers, we further fitted the dynamic structure factor by the Rouse model, with the friction coefficients ξ as fitting parameters. The results are shown in Fig. S11. We only chose $q = 0.05$ in the fitting because such a value of q quantifies the relaxation on the whole-chain level. The corresponding values of the friction coefficients are plotted in Fig. 9 in the main text and are consistent with the values evaluated by the other two methods.

Sticky Rouse Model The original Rouse model describes the relaxation of linear homopolymers. However, in the copolymer system, the dynamics of the chains are obviously influenced by the sequence of dimethyl and diphenyl monomers. If one attempts to incorporate the variation of the friction coefficients of the different monomers explicitly, the sticky Rouse model is useful, although it was originally applied to study associative polymers.¹³⁻¹⁵ The sticky Rouse model has been successfully applied to understand the dynamics of polymers with associative groups that can form transient physical bonds such as in hydrogen bonding, metal-ligand coordination, and $\pi - \pi$ stacking.¹⁶⁻¹⁸ Following the single chain model,¹⁹ the sticky Rouse model describes the motion of an unentangled Gaussian chain as in Eq. S2

$$\xi_0 \Xi \frac{d\mathbf{Q}}{dt} = -K_s \mathbf{Z}\mathbf{Q} + \mathbf{C}\mathbf{F} \quad (\text{S2})$$

where Ξ is a diagonal matrix with its elements $\Xi_{ii} = \xi_i/\xi_0$ being the ratio of friction coefficient for the i^{th} bead with ξ_0 as the reference. \mathbf{C} is a $N_R \times 3$ conversion matrix. \mathbf{Q} is

a matrix that represents the coordinates of all the beads and is defined as Eq. S3

$$\mathbf{Q} = [\mathbf{R}_1 \ \mathbf{R}_2 \ \cdots \ \mathbf{R}_{N_R}]^T \quad (\text{S3})$$

The K_s on the RHS of Eq. S2 is the spring constant of the entropic spring connecting neighboring beads and \mathbf{Z} is the Rouse-Zimm (RZ) matrix, a representation of the connectivity of all the beads of on a polymer chain. In the current study with only the linear chain considered, the RZ matrix is given by Eq. S4

$$\mathbf{Z} = \begin{bmatrix} 1 & -1 & & & \\ -1 & 2 & -1 & & \\ & & \cdots & & \\ & & & -1 & 1 \end{bmatrix} \quad (\text{S4})$$

Finally, the 3×3 matrix \mathbf{F} represents random thermal forces acting on the beads (as in Brownian motion) where its elements $f_{n\alpha}$ follow an ensemble-averaged correlation function as given by Eq. S5. The subscripts n and α are Einstein indices that go from 1 to 3 in the Cartesian coordinate.

$$\langle f_{n\alpha}(t) f_{m\beta}(t') \rangle = 2\xi k_B T \delta_{nm} \delta_{\alpha\beta} \delta(t - t') \quad (\text{S5})$$

Upon diagonalization of Eq. S2, one can solve the time evolution of the normalized coordinates. Correspondingly, the diagonal eigenmatrix $\mathbf{\Lambda}$, with elements given as λ_p , to the matrix $\mathbf{\Xi}^{-1}\mathbf{Z}$ is also derived. The Rouse-like relaxation time τ_p^S (with superscript S for sticky Rouse) for the mode p is given in Eq. S6

$$\tau_p^S = \frac{\xi_b}{K_s \lambda_p} \quad (\text{S6})$$

If the ratio of friction coefficient ξ_i/ξ_b equals unity, the sticky Rouse model degenerates to the regular Rouse model. Moreover, it is worth noting that for both the regular Rouse

model and the sticky Rouse model, the smallest eigenvalues are always equal to zero, which corresponds to the rigid body motion of the chain.²⁰ Thus for a chain of N_R beads, there are $N_R - 1$ nontrivial normal modes.

Diffusion coefficient of the PDMS The derived value of the diffusion coefficient of PDMS (in subsection **3.2**) is based on two works of literature. Because the temperature in our simulation is 550 K, which is artificially high as discussed in the manuscript, there is no experimental data available at this temperature. A Vogel-Fulcher-Tammann (VFT) equation, as in Eq. S7, is thus used to extrapolate available data of $D_{ref} = 1.66 \times 10^{-7}$ cm²/s at 296 K.²¹ The chain length (degree of polymerization) was 50, the same as the setup in our simulation. The value of constant $C = 322.07$ is extracted from the second literature.²² The value was based on dielectric spectra and the molecular weight of the sample was 3510 g/mol, which is very close to the setup in our simulation. Therefore, the extrapolated value of the diffusion coefficient, $D = 3.08 \times 10^{-7}$ cm²/s, at 550 K is calculated. On the other hand, the diffusion coefficient estimated at 298 K, by the MSD shown in Fig. S4 (b), is $D = 9.39 \times 10^{-8}$ cm²/s.

$$\log \frac{D}{D_{ref}} = \frac{C}{T - T_{ref}} \quad (\text{S7})$$

References

- (1) Sides, S. W.; Curro, J.; Grest, G. S.; Stevens, M. J.; Soddemann, T.; Habenschuss, A.; Londono, J. Structure of poly (dimethylsiloxane) melts: Theory, simulation, and experiment. *Macromolecules* **2002**, *35*, 6455–6465.
- (2) Habenschuss, A.; Tsighe, M.; Curro, J. G.; Grest, G. S.; Nath, S. K. Structure of poly (dialkylsiloxane) melts: Comparisons of wide-angle X-ray scattering, molecular dynamics simulations, and integral equation theory. *Macromolecules* **2007**, *40*, 7036–7043.

- (3) Fetters, L.; Lohse, D.; Richter, D.; Witten, T.; Zirkel, A. Connection between polymer molecular weight, density, chain dimensions, and melt viscoelastic properties. *Macromolecules* **1994**, *27*, 4639–4647.
- (4) Tzounis, P.-N.; Anogiannakis, S. D.; Theodorou, D. N. General methodology for estimating the stiffness of polymer chains from their chemical constitution: A single unperturbed chain Monte Carlo algorithm. *Macromolecules* **2017**, *50*, 4575–4587.
- (5) Patrone, P. N.; Dienstfrey, A.; Browning, A. R.; Tucker, S.; Christensen, S. Uncertainty quantification in molecular dynamics studies of the glass transition temperature. *Polymer* **2016**, *87*, 246–259.
- (6) Wang, C.; Fytas, G.; Zhang, J. Rayleigh–Brillouin scattering studies of segmental fluctuations in poly (siloxanes). *The Journal of chemical physics* **1985**, *82*, 3405–3412.
- (7) Babu, G.; Christopher, S.; Newmark, R. Poly (dimethylsiloxane-co-diphenylsiloxanes): synthesis, characterization, and sequence analysis. *Macromolecules* **1987**, *20*, 2654–2659.
- (8) Chou, C.; Yang, M.-H. Structural effects on the thermal properties of PDPS/PDMS copolymers. *Journal of thermal analysis* **1993**, *40*, 657–667.
- (9) Deshpande, G.; Rezac, M. E. Kinetic aspects of the thermal degradation of poly (dimethyl siloxane) and poly (dimethyl diphenyl siloxane). *Polymer Degradation and Stability* **2002**, *76*, 17–24.
- (10) Fox, T. G. Influence of diluent and of copolymer composition on the glass temperature of a polymer system. *Bull. Am. Phys. Soc.* **1952**, *1*, 123.
- (11) Han, J.; Gee, R. H.; Boyd, R. H. Glass transition temperatures of polymers from molecular dynamics simulations. *Macromolecules* **1994**, *27*, 7781–7784.

- (12) Shih, H.; Flory, P. Equation-of-state parameters for poly (dimethylsiloxane). *Macromolecules* **1972**, *5*, 758–761.
- (13) Hansen, D. R.; Shen, M. Viscoelastic retardation time computations for homogeneous block copolymers. *Macromolecules* **1975**, *8*, 343–348.
- (14) Wang, F.; DiMarzio, E. The dynamics of block-copolymer molecules in solution. The free-draining limit. *Macromolecules* **1975**, *8*, 356–360.
- (15) Stockmayer, W.; Kennedy, J. Viscoelastic spectrum of free-draining block copolymers. *Macromolecules* **1975**, *8*, 351–355.
- (16) Rubinstein, M.; Dobrynin, A. V. Solutions of associative polymers. *Trends in Polymer Science* **1997**, *5*, 181–186.
- (17) Zhang, Z.; Chen, Q.; Colby, R. H. Dynamics of associative polymers. *Soft Matter* **2018**, *14*, 2961–2977.
- (18) Shen, Z.; Ye, H.; Wang, Q.; Kröger, M.; Li, Y. Sticky Rouse Time Features the Self-Adhesion of Supramolecular Polymer Networks. *Macromolecules* **2021**, *54*, 5053–5064.
- (19) Jiang, N.; Zhang, H.; Tang, P.; Yang, Y. Linear viscoelasticity of associative polymers: Sticky Rouse model and the role of bridges. *Macromolecules* **2020**, *53*, 3438–3451.
- (20) Eichinger, B. E. Configuration statistics of Gaussian molecules. *Macromolecules* **1980**, *13*, 1–11.
- (21) Leger, L.; Hervet, H.; Auroy, P.; Boucher, E.; Massey, G. *Rheology Series*; Elsevier, 1996; Vol. 5; pp 1–16.
- (22) Hintermeyer, J.; Herrmann, A.; Kahlau, R.; Goiceanu, C.; Rossler, E. Molecular weight dependence of glassy dynamics in linear polymers revisited. *Macromolecules* **2008**, *41*, 9335–9344.

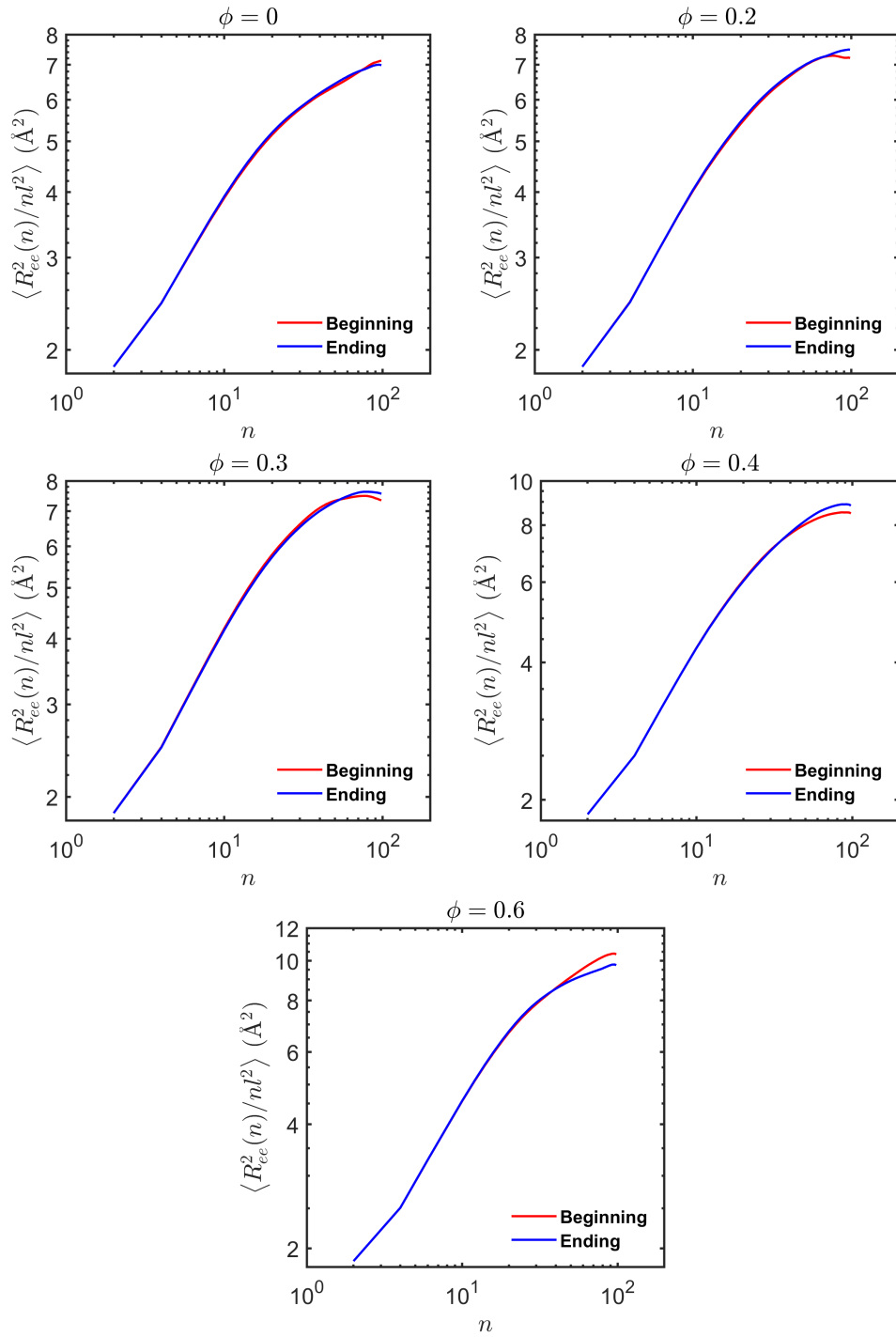


Figure S1: Estimation of the internal mean end-to-end distances.

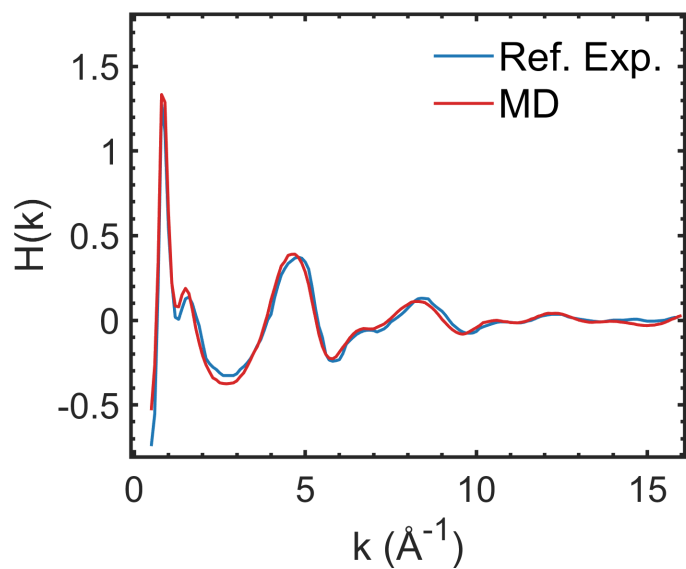


Figure S2: Comparison between the total structure factor calculated from the results of our MD simulation and of experimental measurement.^{1,2}

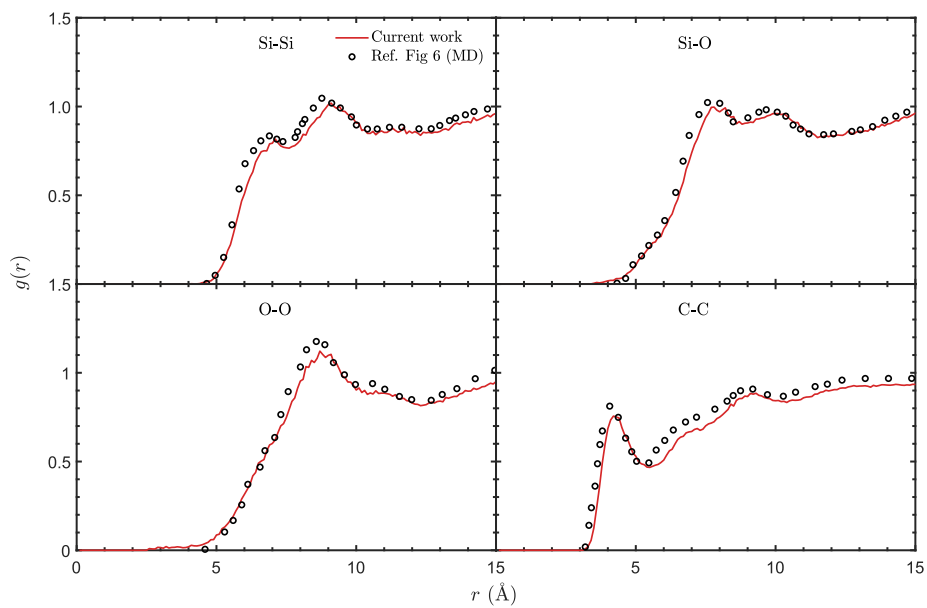


Figure S3: Comparison of the RDFs of PDMS at 300 K with previous study.^{1,2}

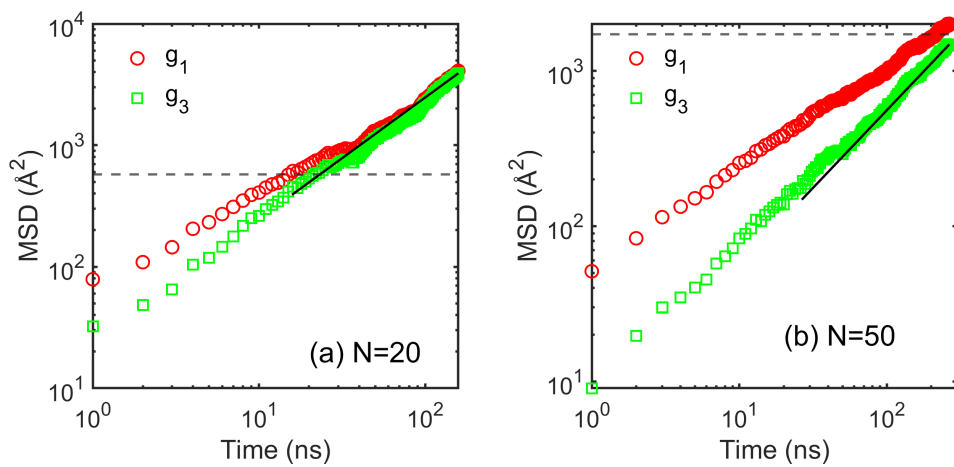


Figure S4: MSD curves for 20- and 50-monomer PDMS at 298 K.

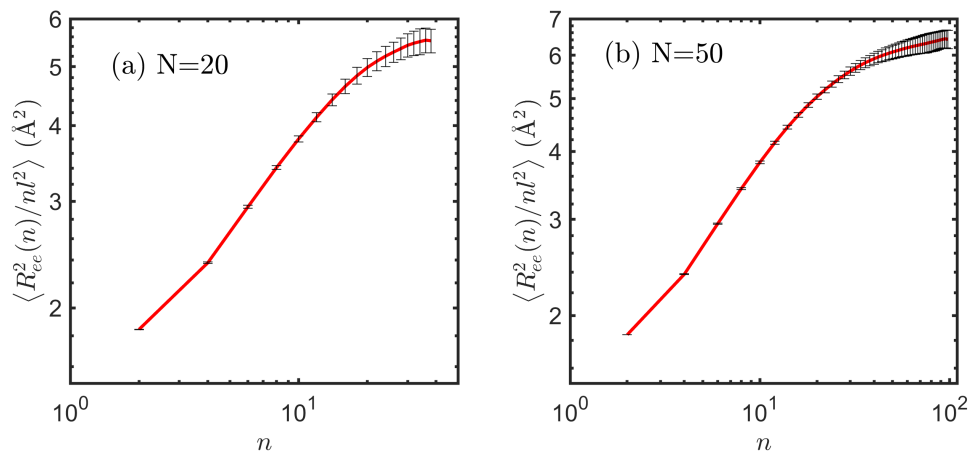


Figure S5: Evaluation of characteristic ratio C of PDMS at 298 K

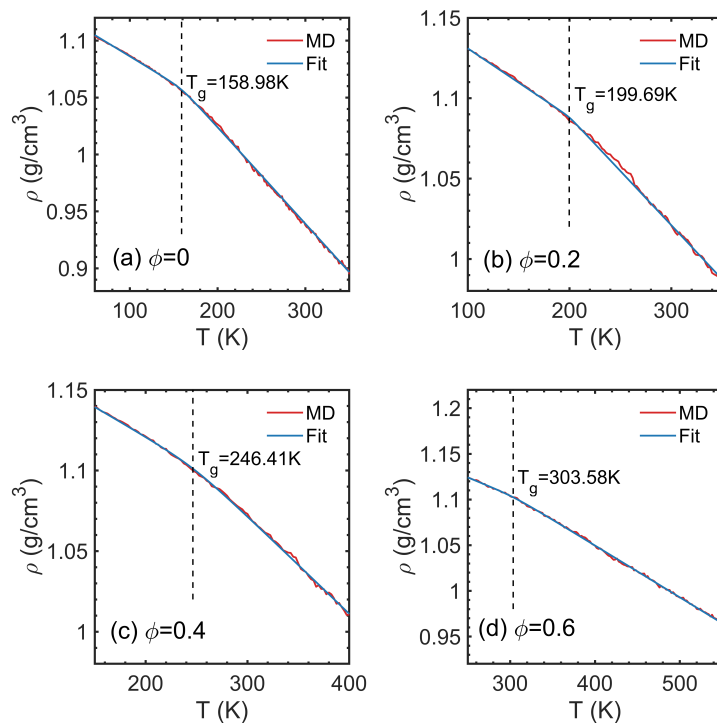


Figure S6: Estimation of the glass transition temperature T_g by annealing from high to low temperature.

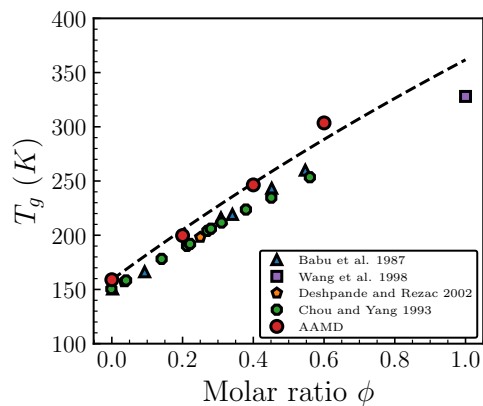


Figure S7: Comparison of the estimated values of T_g with experimental results.⁶⁻⁹

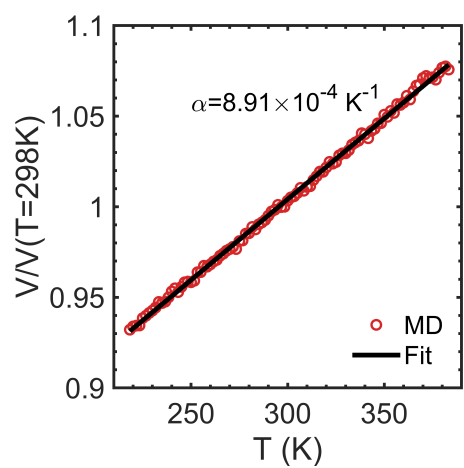


Figure S8: Estimation of the glass transition temperature T_g by annealing from high to low temperature.

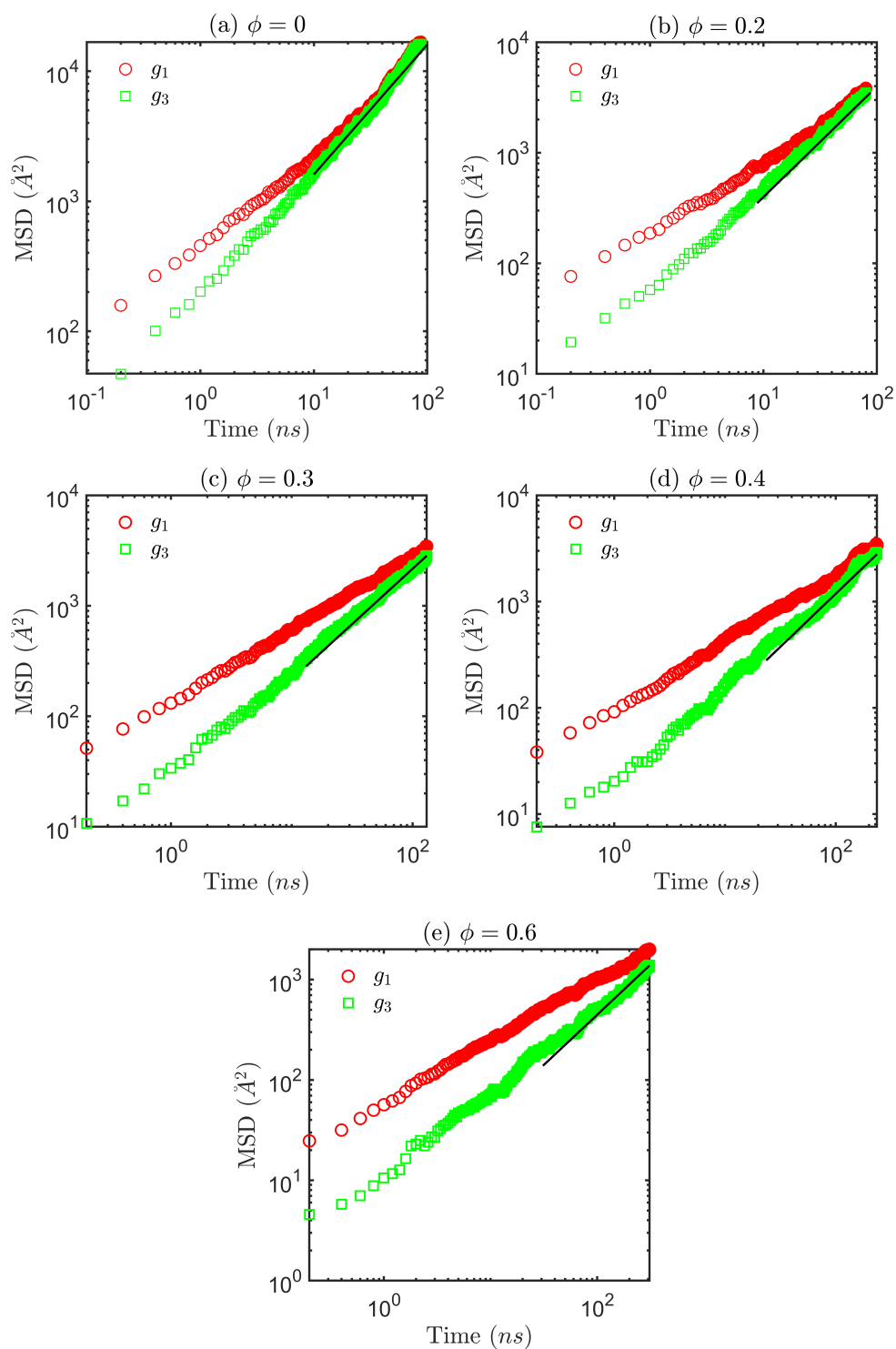


Figure S9: The mean squared displacements of the monomer and the center-of-mass of the polymer chains are detailed. The slope of the dark solid lines is unity, representing the Fickian diffusion regime.

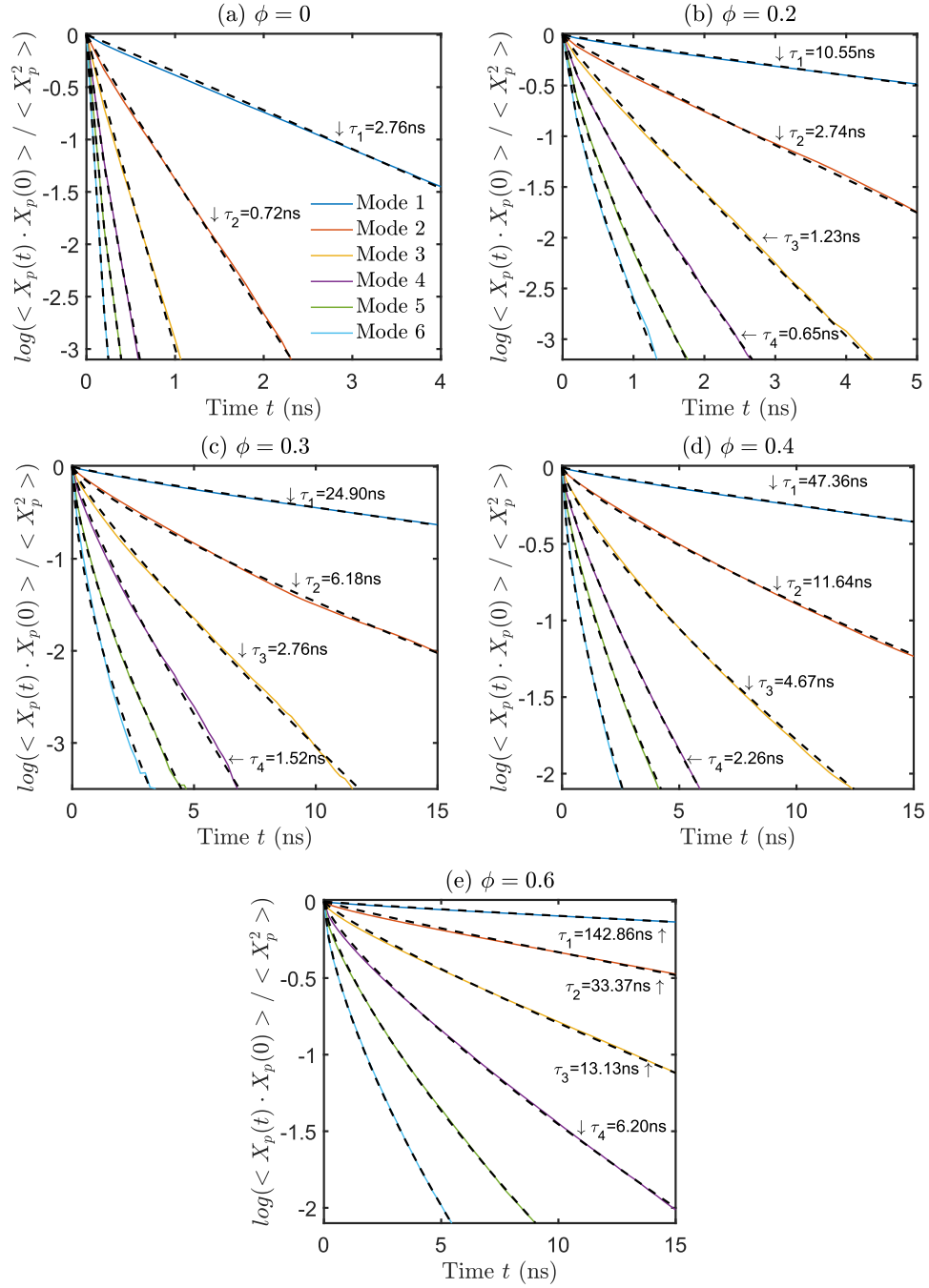


Figure S10: Effective relaxation times according to the autocorrelation of the normal modes.

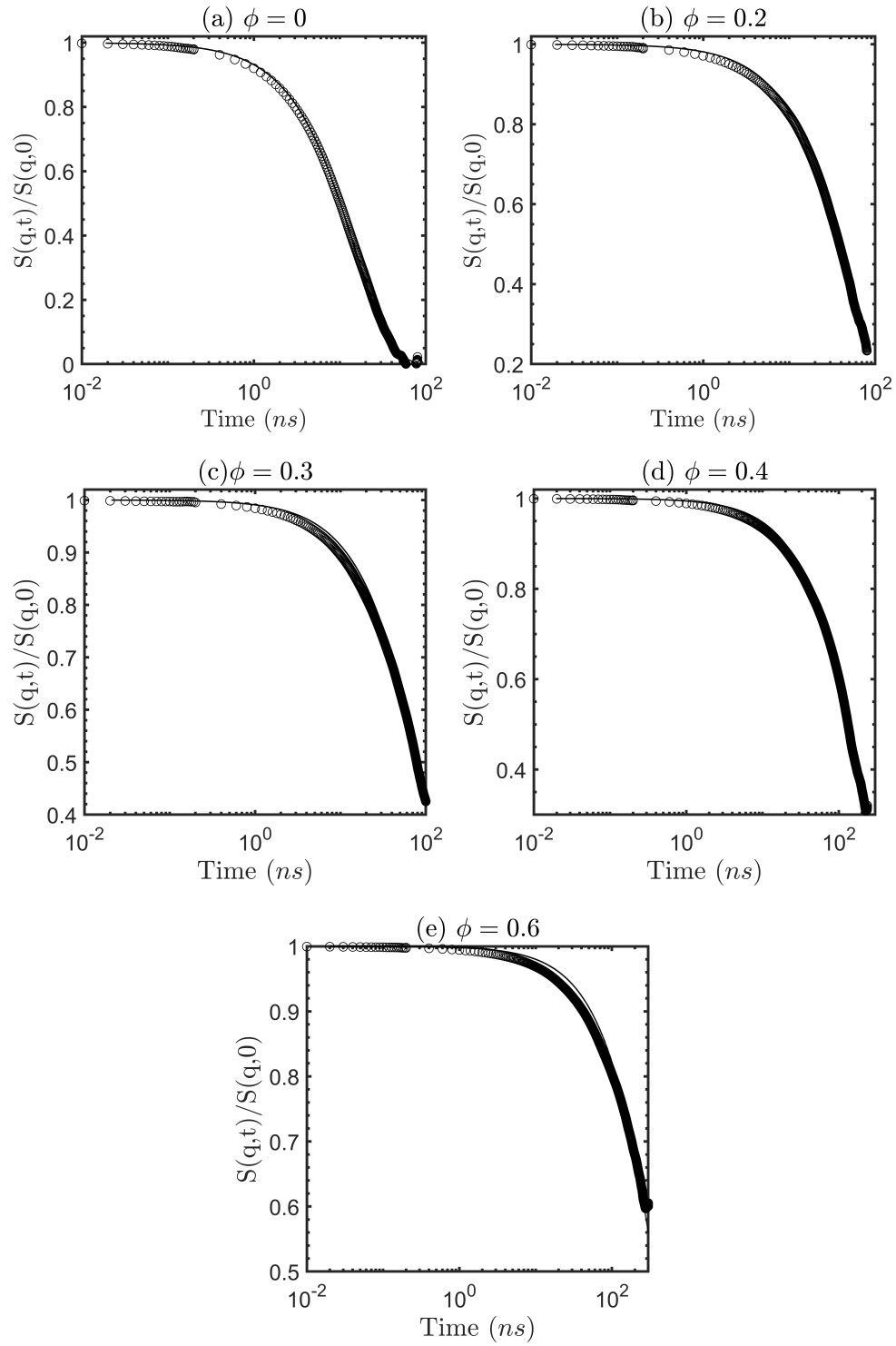


Figure S11: Fitting of the dynamics structure factors. Only the curves of $q = 0.05$ are shown.